Organic & Biomolecular Chemistry

Cite this: *Org. Biomol. Chem.*, 2011, **9**, 1126

www.rsc.org/obc

PAPER

A light-powered stretch–contraction supramolecular system based on cobalt coordinated [1]rotaxane†

Chao Gao, Xiang Ma, Qiong Zhang, Qiaochun Wang, Dahui Qu and He Tian*

Received 22nd September 2010, Accepted 19th October 2010
DOI: 10.1039/c0ob00764a

A mechanically switchable bistable [1]rotaxane, constituted of azobenzene modified cyclodextrins (CyDs) and a Schiff base bridged by a metallosalen unit, was designed and synthesized. ^{1}H NOESY NMR and ICD spectra were investigated to characterize the movement process of this stretch–contraction supramolecular system. The geometries of [1]rotaxane before and after irradiation by UV light were optimized and calculated. Coordinated with cobalt(III) ion, the rotaxane becomes more rigid and linear, which is seen from the more obvious signals in the induced circular dichroism (ICD) and ^{1}H NMR spectra. This type of light-powered [1]rotaxane has favourable repeatability and exhibits a novel approach to elaborate the transformation of a light-driven molecular machine.

Introduction

Supramolecular chemistry, since this basic concept was originated by J. M. Lehn *et al.*,[1] has become a perfect bridge to tightly combine biology and chemistry. Profiting from the elegance and complexity of biological systems,[2] a wealth of inspiration is provided for synthetic chemists. And artificial molecular machines [3] have gradually appeared as one of the emerging fields of chemistry in the past decade. It has a wide range of potential applications in many fields such as molecular wires,[4] molecular memories [5] and logic gates.[6] The construction of molecular engineering attracts a lot of attention from material chemists devoting themselves to build their own nano-empires.

Beginning with the first molecular shuttle synthesized by Stoddart *et al.* in 1990s,[7] molecules or molecular assemblies, for which a certain part can be set into motion deliberately, have triggered great interest as "machines" in the course of years. According to different properties, such as different host–guest systems, and different stimulated manners, the assemblies are divided into different categories. Till now various molecular machines become more complicated and functional.[8] Rotaxanes, as mechanically interlocked molecular architectures, have developed extremely fast in recent years. The first CyD-based [1]rotaxane was synthesized by Easton [9] *et al.* starting from a [2]rotaxane *via* an indirect method by fixing a covalent linkage between the stilbene axis and the CyD rings. Henceforth Harada [10] *et al.* reported that β-CyD derivatives formed self-inclusion complexes in aqueous solution and focused on their dynamic behavior. Recently our group reported a fully optical CyD-based [1]rotaxane *via* self-complementary and Suzuki-coupling capping.[11] Most [1]rotaxanes contain only one macrocycle and a bulky stopper, till now it is rare to use symmetrical structures to form [1]rotaxanes containing two macrocycles. Here we prepare self-assembled β-CyD derivatives connecting with each other *via* metal salen unit to form a novel light-driven [1]rotaxane.

Obviously, photochemical stimulation is one of the valuable choices to be employed in the design of molecular machines. Photochemical responses have self-evident advantages: (1) the systems can be stimulated much more convenient and switched faster; (2) they can work without generating any chemical waste; (3) some suitable optical output signals can be used for detecting (reading) mechanical molecular motions.[12] Stilbene and azobenzene moieties [13] can be photoisomerized efficiently depending on photochemical stimulation, and are widely used in self-assembled systems. More recently a stilbene rotaxane based on cyclodextrin driven by UV light was synthesized by Easton [13c] *et al.* to realize the contraction and extension of a muscle. On the other hand, owing to its high hydrophilicity, low toxicity, and selective recognition towards many model substrates, cyclodextrin [14] as a natural macrocycle has a huge range of applications in drug transportation, biological or pharmic research and biological catalysts.[14b] The cyclodextrin encircling some guests such as the azobenzene moiety can generate induced circular dichroism (ICD) signals,[15] which can be set as an optical output signal to observe the motions of molecular compounds. ICD spectra can undoubtedly monitor the molecular-scale motions much faster and more sensitively when the rotaxane is irradiated by UV light. The introduction of a cobalt ion strengthens the rigidity and linearity of this molecule, which amplifies and regularizes the ICD signals.

Key Laboratory for Advanced Materials and Institute of Fine Chemicals, East China University of Science & Technology, Meilong Road 130, Shanghai 200237, P. R. China. E-mail: tianhe@ecust.edu.cn; Fax: +86-21 64252288

† Electronic supplementary information (ESI) available: Synthetic methods, 2D NMR spectrum, UV-Vis and ICD spectra details. See DOI: 10.1039/c0ob00764a

Here we report the synthesis of a symmetric [1]rotaxane combined with a cobalt(III) ion bridged by Schiff base units [16] as a light-powered molecular machine. We emphasize the performance of the azobenzene moiety and the Schiff base unit before and after UV irradiation in ICD spectra. The [1]rotaxane generates obvious signal changes after UV irradiation which indicated the motion of rotaxane through ICD spectra. β-CyD derivatives possessing functional azobenzene groups and the Schiff units are discussed from the viewpoints of the size/shape matching and induced-fit interaction between the host and guest. ^{1}H NOESY NMR spectra are also employed to characterize the movement process of this [1]rotaxane. This novel light-driven synthetic molecular actuator might be constructed as a potential nano-generator.

Results and discussion

Synthesis and characterization of [1]rotaxane (ASC-Co)

The synthesis of **ASC-Co** was started from the compound mono-6-deoxy-6-(4-aminobenzoyl)-β-CyD (**B**), as illustrated in Scheme 1. **B** was prepared from sodium 4-aminobenzoate and **6-TsO-β-CyD**. **6-Azo-CyD** (**C**) was obtained from **B** and salicylaldehyde in 32% yield. **C** was stirred in aqueous solution for 24 h before reacting with two equivalents of ethyl diamine (**EDA**) to create the [1]rotaxane (**ASC**). After dialysis through a 2000 MWCO cellulose membrane with distilled water (5 L), the pure **ASC** was coordinated with cobalt ion in aqueous solution for 3 h and then gave birth to the target product [1]rotaxane-Co (**ASC-Co**). **C** was assembled with 1-adamantanol firstly to form an inclusion complex after stirring with ten equivalents of 1-adamantanol for 24 h in water solution in order to push the azobenzene unit out of the CyD cavity, then reacted with two equivalents of ethyl diamine (**EDA**) to create the intermediate compound. After this solution was extracted by CH_2Cl_2 to remove the 1-adamantanol, the rest of the procedures for synthesizing compound **RASC-Co** are the same as that of **ASC-Co**.

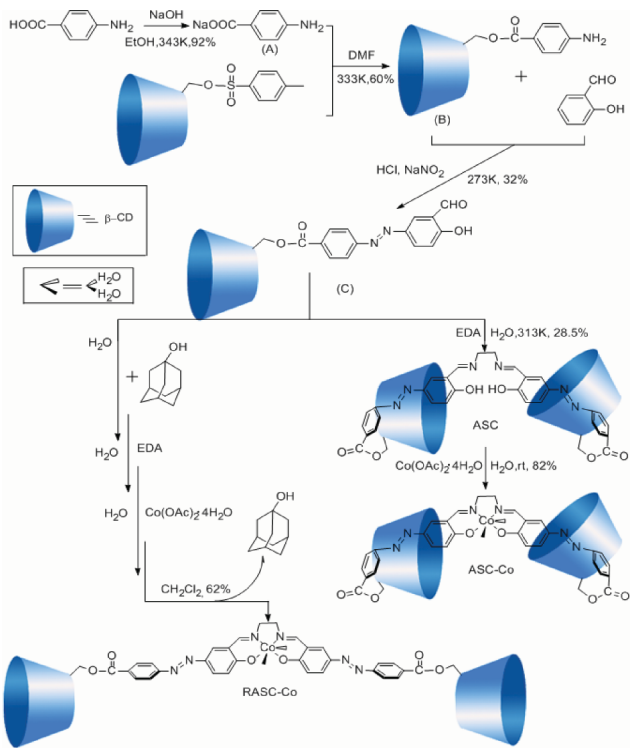

Scheme 1 The synthesis of **RASC-Co**, [1]rotaxane (**ASC**) and [1]rotaxane-Co (**ASC-Co**).

Both **ASC-Co** and the reference compound **RASC-Co** were characterized by means of ^{1}H NMR spectra, ^{1}H NOESY NMR spectra and MALDI-TOF mass spectrometry. Fig. 1 shows the partial ^{1}H NMR spectra (500 MHz) of **ASC-Co** and **RASC-Co** in D_2O (298 K). The chemical shifts of H_c, H_d protons and H_f of the thread decrease by δ = 0.5, 0.17 and 0.21 ppm in the **ASC-Co** with respect to **RASC-Co** and the chemical shifts of $H_{a,a'}$, $H_{b,b'}$ and H_e protons increase by δ = 0.30, 0.15 and 0.22 ppm, respectively. The reasons giving rise to these changes of signals are multiple, and the influence of the β-CyD cavity on the electron cloud density of these protons is the most important, besides, the spatial rotation and twist of the azobenzene moiety plays a role.[17] The MALDI-TOF spectra of **ASC-Co** and **RASC-Co** are similar and both exhibit the same signal at m/z 1451.5, which corresponds to [**ASC-Co** (or **RASC-Co**) + **Na** − H_2O]$^{2+}$ respectively, since the m/z of **RASC-Co** and **ASC-Co** are identical (Figure S1 and S2 in Supporting Information).

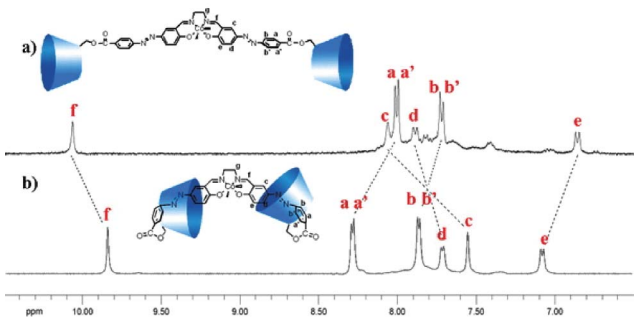

Fig. 1 Partial ^{1}H NMR spectra of **RASC-Co** (a) and **ASC-Co** (b) in D_2O at 25 °C.

The ^{1}H NOESY NMR spectra may supply direct evidence to support the inclusion and response to the relative spatial position. Some protons located close in space can display NOE (Nuclear Overhauser Effect) cross-peaks between the relevant protons in ^{1}H NOESY NMR spectra. The presence of the azobenzene moiety inside the β-CyD cavity in **ASC-Co** has been confirmed by ^{1}H NMR NOESY spectroscopy in aqueous solution. The NOESY spectrum of **ASC-Co** (Fig. 2) displays identifiable NOE cross-peaks between H_3, H_5, H_6 and $H_{6'}$ of β-CyD and H_b, $H_{b'}$ of azobenzene moiety; H_5, H_6 protons of β-CyD and H_a, $H_{a'}$ protons of azobenzene moiety; H_3 proton of β-CyD and H_d, H_e protons of azobenzene moiety. Whereas, the NOE cross-peak between H_2 protons of β-CyD and H_f proton of Schiff base unit also shows clear correlation. H_f proton belongs to the -C═N- group which used to be outside the cavity and forms no signal in the ^{1}H NOESY NMR, but the calculated structure below of **ASC-Co** suggests that the H_f proton is much closer to the H_2 protons of β-CyD which causes the strong NOE cross-peaks.

Compared with the **ASC-Co**, there are no obvious NOE cross-peaks between the H_3 and H_5 protons on the interior of the β-CyD annulus and the aromatic protons in the 2D NOESY spectrum of **RASC-Co** (Figure S3 in SI), indicating the location of the

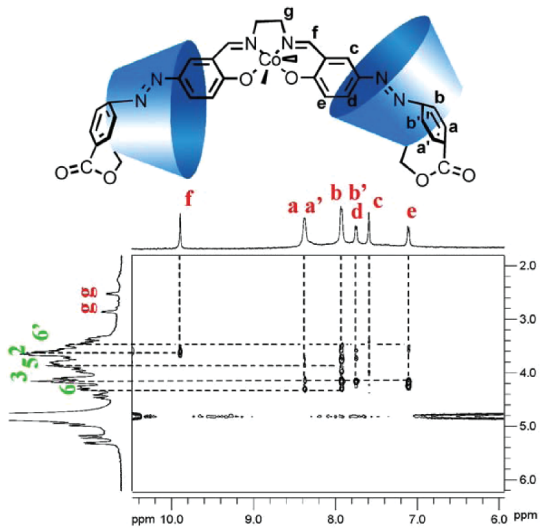

Fig. 2 Partial ^{1}H NOESY NMR spectra of **ASC-Co** in D_2O at 25 °C.

azobenzene moiety above the CyD cavity and the exclusion of the thread out of the CyD cavity, thereby confirming the structures of **ASC-Co** and **RASC-Co**. Besides, NOE cross-peaks between H_g and H_c are found in the ^{1}H NOESY NMR of **ASC** (Figure S4 in SI), however H_g protons of Schiff base unit have no NOE cross-peak with the H_c proton of the azobenzene moiety in the ^{1}H NOESY NMR of **ASC-Co**. The result suggests that after the **ASC** coordinated with cobalt(III) ion, the metallosalen-bridge cannot move freely, and cobalt(III) ion fixes the bridge so tightly that the whole molecule becomes more rigid. As a consequence the NOE cross-peaks intensity of H_c, H_d, H_c protons of azobenzene moiety becomes weaker after coordination compared with the signals in Figure S4, and the azobenzene moiety cannot move further into the cavity of β-CyD. As shown in Figure S5, irradiation of **ASC-Co** at 365 nm for 1 h leads to new sets of NOEs between protons of the azobenzene unit and protons of β-CyD. The cross-peaks of H_{a*}, H_{d*} and H_{c*} protons change when contrasted with the signals before irradiation due to the shift of position. These results indicate that **ASC-Co** undergoes photoisomerization and the azobenzene unit changes from *trans* to *cis* and generates some new chemical shifts. The H_a and H_b protons somehow move outside or near the narrow rim of β-CyD, in the meantime H_c, H_d and H_c protons are drawn into the cavity of β-CyD.

Contraction motion with photoisomerization

The *E*/*Z* photoisomerization process of **ASC-Co** in D_2O is investigated by monitoring the changes in relative ^{1}H NMR spectra. The ^{1}H NMR spectra can provide direct evidence to prove the variety of positions of **ASC-Co**: the chemical shifts of the new protons are revealed because of their different chemical environments. To validate these hypotheses, the azobenzene-based **ASC-Co** was irradiated by the UV light to induce its *E*/*Z* photoisomerization.

As expected and shown in Fig. 3b, irradiation by the UV light at 365 nm for 1 h leads to some new signals for *cis*-**ASC-Co**, appearing at δ = 10.26 (H_{f*}), 7.94 (H_{a*}, H_{c*}, H_{d*}), 6.90 (H_{e*}) and 6.75 (H_{b*}) ppm, corresponding to the initial peaks of *trans*-**ASC-Co** appearing at δ = 9.91 (H_f), 8.39 ($H_{a,a'}$), 7.75 (H_d), 7.60 (H_c),

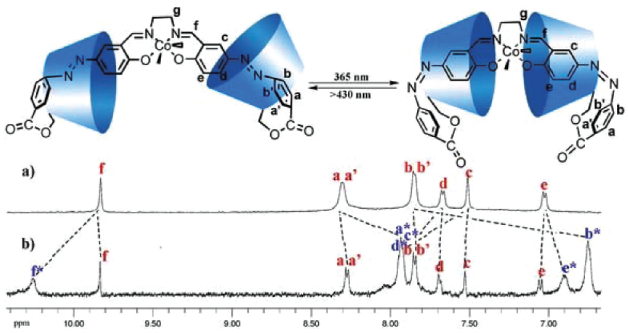

Fig. 3 Partial ^{1}H NMR spectra of **ASC-Co** in the original state (a) and in the photostationary state (b) after irradiation by 365 nm for 1 h in D_2O.

7.13 (H_c) and 7.93 ($H_{b,b'}$) ppm, respectively. The signals of H_{a*} and H_{b*} protons are up-field shifted ($\Delta\delta$ up to 0.45 and 1.18 ppm) with respect to the original positions, and other protons are also shifted compared with their initial positions. It is reasonable that the aromatic protons signals of the azobenzene moiety are generally shifted upon their isomerization from *trans* to *cis* configuration, as a result of a complex effect of relative spatial configuration changes and magnetic shielding effect caused by the aromatic rings in the other half of azobenzene unit when the two aromatic rings close. Integrals of the two signals for H_f and H_{f*} protons appear with a 1 : 2 ratio, which suggests that, at the photostationary state, about 67% of *trans*-**ASC-Co** transformed to the *cis*-**ASC-Co**. The ratio of photoisomerization inferred that due to the transformation of azobenzene moieties from *trans* to *cis*, the two rings crowded together and shorten the whole molecule.

ICD spectrum as a notable output signal becomes a convenient and widely employed method for the elucidation of the absolute conformation of chiral organic compounds. ICD experiments on **ASC**, **ASC-Co** and **RASC-Co** (1.2×10^{-4} mol dm^{-3}) are carried out in order to contrast and monitor the stretch or contraction of the supramolecular system in aqueous solution at 25 °C.

With knowledge of previous investigations [18] on the ICD properties of cyclodextrin modified structures, the positive/negative ICD signal can be observed once the electric transition dipole moment of the guest inside the host cavity is aligned parallel/perpendicular to the axis of cyclodextrin. On the other hand, the ICD signal is dramatically reversed when the electric transition moment of the guest is outside the host cavity. Whereas the ICD signal turns to zero if the angle between the transition moment and the CyD axis is about 54.7°.[18c] Above all, the signal of ICD can supply proper evidence to testify to the spatial position between the host and the guest.

Firstly the differences of ICD signals between **RASC-Co** and **ASC-Co** were compared. As seen from Figure S8, the ICD spectrum of **RASC-Co** in aqueous solution shows that a wide negative Cotton effect peak and wide positive Cotton effect peak rise at 450 nm and 350 nm irregularly. On the contrary, the ICD signal of **ASC-Co** is obvious and regular under comparable conditions. According to Harata, Kajtár and Nau's sector rule on the ICD phenomena of β-CyD complexes, we can deduce that the azobenzene and Schiff base moieties in these compounds in the range of 220–550 nm are induced by two allowed transitions perpendicular to each other. That is to say, the peaks in the ICD spectra (Fig. 4) respectively belong to four electric transition dipole moments: π–π*, n–π* of the azobenzene moiety and π–π*, n–π*

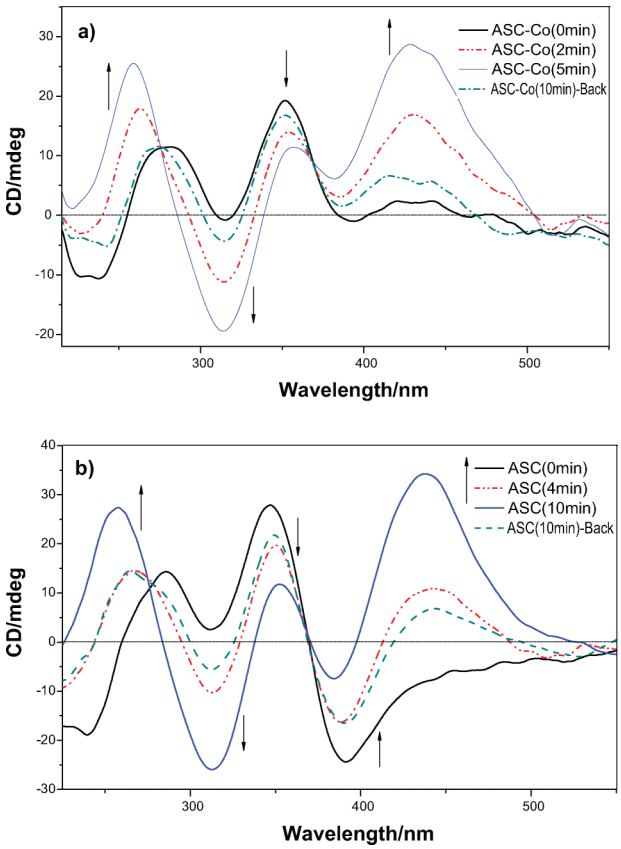

Fig. 4 ICD spectra changes for **ASC-Co** (a) and **ASC** (b) (25 °C, 1.2×10^{-4} mol dm^{-3}) in aqueous solution by irradiation at 365 nm. And the spectra changes shift back to a large extent by irradiation at 430 nm [Line **ASC-Co** (10 min)-back and b (10 min)-back].

of the Schiff base unit. In Fig. 4a, the ICD spectrum of **ASC-Co** shows a negative Cotton effect peak at 232 nm, and two positive Cotton effect peaks at around 281 nm and 352 nm. Upon irradiation with UV light of 365 nm for 10 min, two new strong positive Cotton effects increase at around 259 nm, 431 nm and a strong negative cotton effects at 314 nm reveals gradually.

The geometries of *trans*- and *cis*-**ASC-Co** (Fig. 6 below) and **RASC-Co** shaft (Figure S6) were optimized with the hybrid density functional method B3LYP [19] using the Gaussian 03 [20] program. The calculations were performed by using the effective core pseudopotentials (ECP) basis set on the Co(III) ion, and the standard basis set 3-21G for carbon, oxygen, nitrogen, and hydrogen atoms. The Ne core electrons of Co were replaced by an ECP and DZ quality Hay and Wadt Los Alamos ECP basis set (LANL2DZ) [21] was used for the valence electrons. In Fig. 6, when the hydrogen bond exists, it can be seen that after irradiation by UV light at 365 nm, the azobenzene units photoisomerized from *trans* to *cis* and the two cyclodextrins move closer together, accompanied by the contraction of the shaft into an "M" type due to the hydrogen bonding interaction formed between the two cyclodextrins. By contrast, the conformation of the shaft (Figure S6 in SI) near the Co(III) coordination center hardly changes due to the isomerization, which emphasizes the role of hydrogen bonds between two cyclodextrins to shrink the molecule. The length of **ASC-Co** changes from 26.06 Å in *trans*-status to 19.49 Å in *cis*-status ($\Delta L = 6.57$ Å). Besides the hydrogen bond as a main factor to influence the transformation, the force from photoisomerization also plays a critical role as two strong arms to drive the two cyclodextrins to be close and far apart.

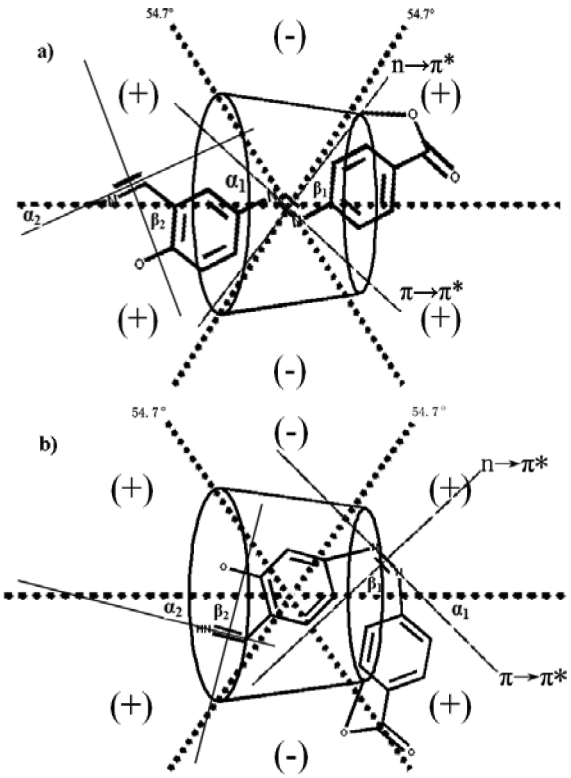

Fig. 5 Relationship of the angles α_1, β_1, α_2, β_2 and positions between the β-CyD ring and the linear subunit before (a) and after (b) the photoisomerization of the azobenzene moiety and the Schiff base unit in H_2O about **ASC-Co**. α_1, α_2 are the angles between the axis and the orientation of $\pi\rightarrow\pi^*$ transition which are separately belong to azobenzene moiety and Schiff base unit while β_1, β_2 are the angles between the axis and the orientation of $n\rightarrow\pi^*$ transition.

In addition, Fig. 6 shows that azobenzene and Schiff base units are both encircled by the cavity of cyclodextrin after irradiation at around 365 nm, while the azobenzene moiety is the only one unit which is almost in the cavity of β-CyD before irradiation. In the Fig. 4a, the ICD signals of the Schiff base unit containing $n\rightarrow\pi^*$ transition and $\pi\rightarrow\pi^*$ transition have red-shifts of about 26 nm and 34 nm, respectively.

The angles of the four transitions are used to assist with the ICD spectra analysis. As Fig. 5a shows, β_1 is supposed to be the angle which causes the signal at around 431 nm to be nearly zero. The $\pi\rightarrow\pi^*$ transition of the azobenzene moiety generates a positive cotton effect peak that is ascribed to α_1. On the contrary, the Schiff base unit is outside the cavity of β-CyD and $n\rightarrow\pi^*$ the transition of the Schiff base unit generates a positive Cotton effect peak at 281 nm, whereas the $\pi\rightarrow\pi^*$ transition of the Schiff case unit gives rise to a negative Cotton effect. As mentioned above, the azobenzene moieties in **ASC-Co** are deep inside the β-CyD cavity with an acclivitous orientation. After irradiation by 365 nm for 10 min, the azobenzene moiety changes from *trans*-status to *cis*-status. As a consequence the Schiff base unit is forced to be dragged into the cavity to cause the spectrum signal to change substantially. With the location of the Schiff base unit moving from outside to

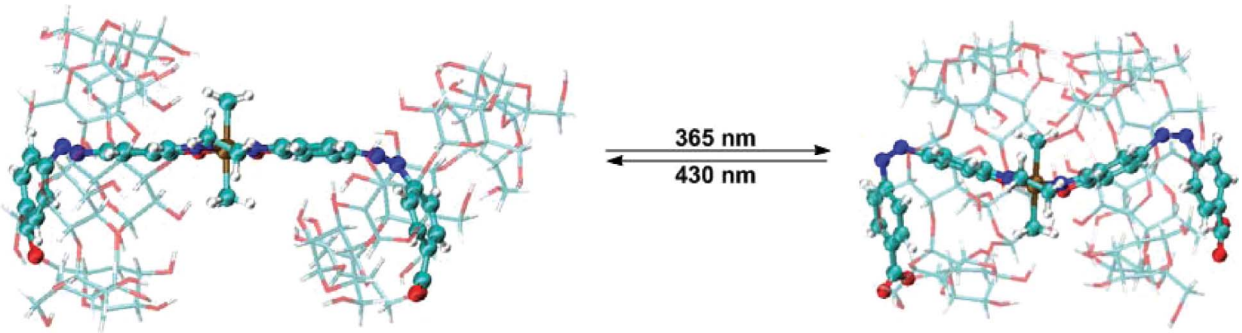

Fig. 6 Calculated structures of **ASC-Co** from *trans*- to *cis*-form after the irradiations.

inside gradually, the signals reverse relatively. From Fig. 5b, the Schiff base unit enters the cavity to cause a negative Cotton effect which is larger than the positive one before, and a positive Cotton effect peak. Meanwhile, azobenzene moieties cause other changes of spectrum at the wavelength range between 350 nm and 500 nm.

Compared with the ICD spectrum of **ASC-Co**, the ICD spectrum of **ASC** has some discernable differences (Fig. 4). One of distinct differences is an extra negative cotton effect at around 392 nm. After irradiation by UV light at 365 nm, the negative cotton effect peak at 392 nm decreases meanwhile a positive cotton effect arises at 430 nm concomitantly. As shown in Figure S6 in SI, the structure does not have absolute mirror-symmetry as we presumed. The angle of the metallosalen somehow twists against each other due to the steric hindrance. When the azobenzene moiety of **ASC** transformed from the *trans*- to *cis*-form, the azobenzene moiety doesn't go towards the outside firstly but shrinks into the cavity of β-CyD. Without the ion combining with the Schiff base, the shaft with which the β-CyD glides along is longer than **ASC-Co**. This means it can provide much more space for β-CyD to move, which makes the azobenzene moiety near to the narrow rim. Owing to the relative spatial position, the azobenzene moiety compresses to the center when transforming. As the bond vibrates, the unit moves and vibrates towards the outside. The signal changes from a negative cotton effect to a positive cotton effect and red-shifts about 40 nm. The ICD signals of the Schiff base unit are similar to that of **ASC-Co**. The spectrum of **ASC** without metal coordination is not as regular as the one of **ASC-Co**.

With respect to the UV/Vis spectroscopy experiments, we compared the absorption spectra of **ASC-Co** with **RASC-Co** in Fig. 7a, which shows that the absorption value of **ASC-Co** has a blue shift from 372 nm to 352 nm ($\Delta\lambda$ = 20 nm) and the intensity of absorption was weaker after the azobenzene moieties embedded in the cavity of β-CyD. And Fig. 7b provides some details to characterize the motion of this machine. For **ASC-Co**, after irradiation upon 365 nm, the absorption intensity of the azobenzene moiety degenerates from 0.41 to 0.27. Whereas, the absorption peak of the Schiff base unit strengthens from 0.45 to 0.46 with about an 11 nm red-shift concomitantly. It is attributed to the photoisomerization of the azobenzene moieties. When **ASC-Co** reaches to its photostationary state, a decrease in absorption at around 348 nm (ΔA = 0.14) and an increase in absorption at around 240 nm (ΔA = 0.01) happen. After irradiation by 430 nm for ten minutes, about 70.2% *cis*-**ASC-Co** transformed back to the *trans*-**ASC-Co** according to Fig. 7b, which

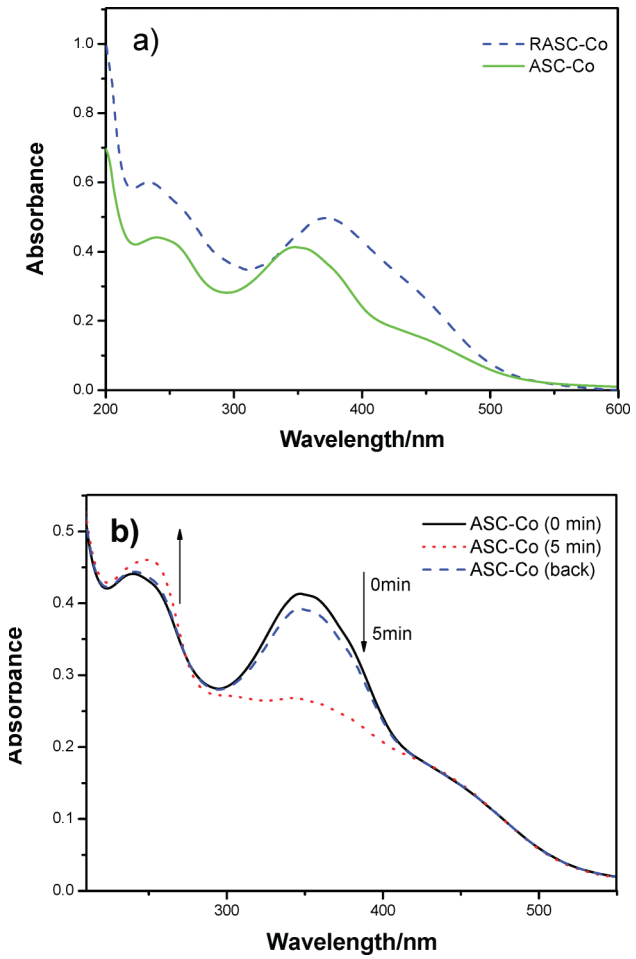

Fig. 7 **(a)** UV/Vis absorption spectra of **RASC-Co** (dash) and **ASC-Co** (solid); (b) the absorption spectra of **ASC-Co** (1.1×10^{-5} mol dm^{-3}) in H_2O at 298 K before (solid), after (dash) irradiation at 365 nm for 5 min and after (dot) irradiation at 430 nm for 10 min.

exhibits good reversibility again. Compared with the UV/Vis spectroscopy spectra between **ASC-Co** and **ASC** (Figure S9 in SI), it can be seen that the UV absorption intensity of the azobenzene moiety slightly degenerates after combining with cobalt(III) ion, besides, the absorption peak of Schiff base unit at 239 nm is more distinct after combining with cobalt(III) ion. All of the spectra demonstrate the fact that **ASC-Co** and **ASC** both have favorable photoisomerization properties, moreover the greater rigidity and

linearity of the compounds through combining with the cobalt(III) ion encourages the regulation of the signals.

Since [1]rotaxane is one of the most crucial targets, the quantity of repeatability is measured. Since the azobenzene derivative has good photoreversibility, the photochemical process of the **ASC-Co** is highly reproducible over more than five cycles (Fig. 8). Moreover, the molecular machine is amazingly stable even preserved in aqueous solution for one month, when the repeatability is the same as initially.

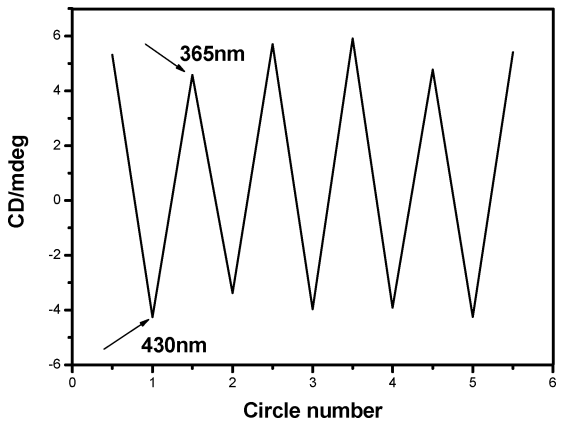

Fig. 8 The Cotton effect peak of **ASC-Co** (at 390 nm) on conducting five optical irradiation switching cycles.

Besides investigating the motion of **ASC-Co** and **ASC**, the optical spectroscopy of compound **C** is also observed and it showed large differences in both UV/Vis and ICD spectra compared with **RASC-Co** and **ASC-Co**. The n→π* transition and π→π* transition give rise separately to a positive cotton effect and a negative cotton effect at 459 nm and 389 nm in ICD spectrum (Figure S10 and S11 in SI). Because the biggest absorbance wavelength is more than 411 nm as shown in the UV/Vis spectrum, it did not represent any distinctly regular change in either the intensity or the wavelength after irradiation by 365 nm for even 1 h. After the aldehyde group reacts with ethyl diamine, the absorption peak will move to 361 nm which is less than the absorption peak of **C**. It shows that the Schiff base unit employs a remarkable role in this supramolecular system.

Conclusions

In summary, a novel light-driven [1]rotaxane based on cyclodextrins and azobenzene moieties has been constructed and showed unique movements. ^{1}H NMR spectroscopic experiments reveal clearly that the transformation of azobenzene moieties from *trans*- to *cis*- can cause the whole [1]rotaxane to contract or extend along with the thread components when irradiated by UV light, which causes the azobenzene moiety to move deep into the cavity of β-CyD and the Schiff unit begin to enter the cavity of β-CyD. As a consequence, two units shuttle through the cavity of β-CyD commutatively leaving obvious tracks in ICD spectra after irradiation by 365 nm and 430 nm, respectively. The changes of ICD spectra are highly distinct as the output signal to monitor the motions of the machine, and theoretical calculated structures vividly describe the movement and the shape changes (from "linear" type to "M" type). Combining with cobalt(III) ion increases the rigidity of the whole compound and induces more regular signals in the ICD spectra. The ASC-Co containing Schiff base unit, a part of which is a notable catalyst in biochemistry, will bring more potential applications. A logical development by replacing the chemically driven redox process with optical stimulations would contribute to a technological basis for the production of a new class of molecular scale devices based upon nanomechanical motion in switchable interlocked molecules.

Acknowledgements

C. Gao and X. Ma contributed equally to this work. This work is financially supported by National Basic Research 973 Program (2011CB808400), NSFC/China (20972053 & 20802019), X. Ma thanks the support from the Fundamental Research Funds for the Central Universities (WJ0911001), the Ph.D. Programs Foundation of Ministry of Education of China (200802511029) and the 'Chen Guang' project supported by Shanghai Municipal Education Commission and Shanghai Education Development Foundation. C. G. is grateful for discussions with Ms. Ruyi Sun, Mr. Liangliang Zhu.

Notes and references

1 J.-M. Lehn, *Supramolecular Chemistry*, VCH: Weinheim,Germany, 1995; V. Balzani, M. Venturi and A. Credi *Molecular Devices and Machines*, VCH. Weinheim, Germany, 2008.
2 P. G. Clark, M. W. Day and R. H. Grubbs, *J. Am. Chem. Soc.*, 2009, **131**, 13631–13633.
3 (*a*) Y.-L. Zhao and J. F. Stoddart, *Langmuir*, 2009, **25**, 8442–8446; (*b*) V. Balzani, A. Credi, F. M. Raymo and J. F. Stoddart, *Angew. Chem., Int. Ed*, 2000, **39**, 3348–3391; (*c*) G. Wenz, B.-H. Han and A. Müller, *Chem. Rev.*, 2006, **106**, 782–817; (*d*) R. E. Dawson, S. F. Lincoln and C. J. Easton, *Chem. Commun.*, 2008, 3980–3982; (*e*) J. F. Stoddart, *Chem. Soc. Rev.*, 2009, **38**, 1802–1820; (*f*) J. D. Crowley, S. M. Goldup, A.-L. Lee, D. A. Leigh and R. T. McBurney, *Chem. Soc. Rev.*, 2009, **38**, 1530–1541; (*g*) A. W. Feinberg, A. Feigel, S. S. Shevkoplyas, S. Sheehy, G. M. Whitesides and K. K. Parker, *Science*, 2007, **317**, 1366–1370; (*h*) X. Ma and H. Tian, *Chem. Soc. Rev.*, 2010, **39**, 70–80; (*i*) H. Tian and Q.-C. Wang, *Chem. Soc. Rev.*, 2006, **35**, 361–374.
4 (*a*) P. N. Taylor, M. J. O'Connell, A. L. McNeill, M. J. Hall, R. T. Aplin and H. L. Anderson, *Angew. Chem., Int. Ed.*, 2000, **39**, 3456–3460; (*b*) F. Cacialli, J. S. Wilson, J. J. Michels, C. Daniel, C. Silva, R. H. Friend, N. Severin, P. Samori, J. P. Rabe, M. J. O'Connell, P. N. Taylor and H. L. Anderson, *Nat. Mater.*, 2002, **1**, 160–164; (*c*) J. J. Michels, M. J. O'Connell, P. N. Taylor, J. S. Wilson, F. Cacialli and H. L. Anderson, *Chem.–Eur. J.*, 2003, **9**, 6167–6176; (*d*) E. Katz and I. Willner, *Angew. Chem., Int. Ed.*, 2004, **43**, 6042–6108; (*e*) C. A. Schalley, K. Beizai and F. Vögtle, *Acc. Chem. Res.*, 2001, **34**, 465–476.
5 (*a*) M. Cavallini, F. Biscarini, S. Léon, F. Zerbetto, G. Bottari and D. A. Leigh, *Science*, 2003, **299**, 531; (*b*) D.-H. Qu, Q.-C. Wang, J. Ren, K.-C. Chen and H. Tian, *Angew. Chem., Int. Ed.*, 2004, **43**, 2661–2665; (*c*) J. Zhang, W. Tan, X. Meng and H. Tian, *J. Mater. Chem.*, 2009, **19**, 5726–5729; (*d*) H. Zhang, Q. Wang, M. Liu, X. Ma and H. Tian, *Org. Lett.*, 2009, **11**, 3234–3237.
6 (*a*) C. P. Collier, E. W. Wong, M. Belohradsky, F. M. Raymo, J. F. Stoddart, P. J. Kuekes, R. S. Williams and J. R. Heath, *Science*, 1999, **285**, 391–394; (*b*) D. A. Leigh, M. Á F. Morales, E. M. Pérez, J. K. Wong, C. G. Saiz, A. M. Slawin, A. J. Carmichael, D. M. Haddleton, A. M. Brouwer, W. J. Buma, G. W. Wurpel, S. Léon and F. Zerbetto, *Angew. Chem., Int. Ed.*, 2005, **44**, 3062–3067; (*c*) D. –H. Qu, Q.-C. Wang and He Tian, *Angew. Chem., Int. Ed.*, 2005, **44**, 5296–5299; (*d*) D.-H. Qu, F.-Y. Ji, Q.-C. Wang and H. Tian, *Adv. Mater.*, 2006, **18**, 2035–2038; (*e*) R. Ballardini, P. Ceroni, A. Credi, M. T. Gandolfi, M. Maestri, M. Semararo, M. Venturi and V. Balzani, *Adv. Funct. Mater.*, 2007, **17**, 740–750; (*f*) M. Yuan, W. Zhou, X. Liu, M. Zhu, J. Li, X. Yin, H. Zheng, Z. Zuo, C. Ouyang, H. Liu, Y. Li and D. Zhu, *J. Org. Chem.*, 2008, **73**, 5008–5014.

7 P. L. Anelli, N. Spencer and J. F. Stoddart, *J. Am. Chem. Soc.*, 1991, **113**, 5131–5133.
8 (*a*) H. Deng, M. A. Olson, J. F. Stoddart and O. M. Yaghi, *Nat. Chem.*, 2010, **2**, 439–443; (*b*) A. M. Stadler, J. Ramírez and J. M. Lehn, *Chem. Eur. J.*, 2010, **16**, 5369–5378; (*c*) D.-H Qu and B. L. Feringa, *Angew. Chem., Int. Ed.*, 2010, **49**, 1107–1110; (*d*) Y. Li, K. M. Müllen, T. D. W. Claridge, P. J. Costa, V. Felix and P. D. Beer, *Chem. Commun.*, 2009, 7134–7136; (*e*) J. A. Faiz, V. Heitz and J. P. Sauvage, *Chem. Soc. Rev.*, 2009, **38**, 422–442.
9 C. J. B. H Onagi, C. J. Easton and S. F. Lincoln, *Chem.–Eur. J.*, 2003, **9**, 5978–5988.
10 Y. Inoue, M. Miyauchi, H. Nakajima, Y. Takashima, H. Yamaguchi and A. Harada, *J. Am. Chem. Soc.*, 2006, **128**, 8994–8995.
11 X. Ma, D. Qu, F. Ji, Q. Wang, L. Zhu, Y. Xu and H. Tian, *Chem. Commun.*, 2007, 1409–1411.
12 B. K. Juluri, A. S. Kumar, Y. Liu, T. Ye, Y.-W. Yang, A. H. Flood, L. Fang, J. F. Stoddart, P. S. Weiss and T. J. Huang, *ACS Nano*, 2009, **3**, 291–300.
13 (*a*) X. Ma, Q.-C. Wang, D.-H Qu, Y. Xu, F.-Y. Ji and H. Tian, *Adv. Funct. Mater.*, 2007, **17**, 829–837; (*b*) Y. Wang, N. Ma, Z. Wang and X. Zhang, *Angew. Chem., Int. Ed.*, 2007, **46**, 2823–2826; (*c*) R. E. Dawson, S. F. Lincoln and C. J. Easton, *Chem. Commun.*, 2008, 3980–3982; (*d*) S. Tsuda, Y. Aso and T. Kaneda, *Chem. Commun.*, 2006, 3072–3074.
14 (*a*) L. Zhu, X. Li, F.-Y. Ji, X. Ma, Q.-C. Wang and H. Tian, *Langmuir*, 2009, **25**, 3482–3486; (*b*) S.-P. Tang, Y.-H. Zhou, H.-Y. Chen, C.-Y. Zhao, Z.-W. Mao and L.-N. Ji, *Chem. Asian. J.* 2009, *4*, 1354–1360; (*c*) X. Ma, Q. Wang and H. Tian, *Tetrahedron Lett.*, 2007, **48**, 7112–7116; (*d*) A. G. Cheetham, T. D. W. Claridge and H. L. Anderson, *Org. Biomol. Chem.*, 2007, **5**, 457–462; (*e*) L. Zhu, D. Zhang, D. Qu, Q. Wang, X. Ma and H. Tian, *Chem. Commun.*, 2010, **46**, 2587–2589.
15 (*a*) Y. Liu, Y.-L. Zhao, H.-Y. Zhang, Z. Fan, G.-D. Wen and F. Ding, *J. Phys. Chem. B*, 2004, **108**, 8836–8843; (*b*) Y. Liu, Y.-L. Zhao, H.-Y. Zhang, X.-Y. Li, P. Liang, X.-Z. Zhang and J.-J. Xu, *Macromolecules*, 2004, **37**, 6362–6369; (*c*) Y. Liu, H. Wang, H.-Y. Zhang and P. Liang, *Chem. Commun.*, 2004, 2266–2267; (*d*) H. Murakami, A. Kawabuchi, K. Kotoo, M. Kunitake and N. Nakashima, *J. Am. Chem. Soc.*, 1997, **119**, 7605–7606.
16 (*a*) L. Fabbrizzi, M. Licchelli, A. M. Manotti Lanfredi, O. Vassalli and F. Ugozzoli, *Inorg. Chem.*, 1996, **35**, 1582–1589; (*b*) R. M. Haak, S. J. Wezenberg and A. W. Kleij, *Chem. Commun.*, 2010, **46**, 2713–2723.
17 (*a*) P. V. Demarco and A. R Thakkar, *J. Chem. Soc. D*, 1970, 2; (*b*) H.-J. Schneider, F. Hacket, V. Rudiger and H. Ikeda, *Chem. Rev.*, 1998, **98**, 1755–1786; (*c*) G. Fronza, A. Mele, E. Redenti and P. Ventura, *J. Org. Chem.*, 1996, **61**, 909–914; (*d*) H. Xing, S.-S. Lin, P. Yan, J.-X. Xiao and Y.-M. Chen, *J. Phys. Chem. B*, 2007, **111**, 8089–8095.
18 (*a*) M. Kodaka, *J. Phys. Chem.*, 1991, **95**, 2110–2112; (*b*) M. Kodaka, *J. Am. Chem. Soc.*, 1993, **115**, 3702–3705; (*c*) M. Kodaka, *J. Phys. Chem. A*, 1998, **102**, 8101–8103; (*d*) L. L. Zhu, X. Ma, F. Y. Ji, Q. C. Wang and H. Tian, *Chem.–Eur. J.*, 2007, **13**, 9216–9222.
19 (*a*) A. D. Becke, *J. Chem. Phys.*, 1993, **98**, 5648–5652; (*b*) A. D. Becke, *Phys. Rev. A: At., Mol., Opt. Phys.*, 1988, **38**, 3098–3100.
20 M. J. Frisch, G. W. Trucks, H. B. Schlegel, G. E. Scuseria, M. A. Robb, J. R. Cheeseman, Jr. J. A. Montgomery, T. Vreven, K. N. Kudin, J. C. Burant, J. M. Millam, S. S. Iyengar, J. Tomasi, V. Barone, B. Mennucci, M. Cossi, G. Scalmani, N. Rega, G. A. Petersson, H. Nakatsuji, M. Hada, M. Ehara, K. Toyota, R. Fukuda, J. Hasegawa, M. Ishida, T. Nakajima, Y. Honda, O. Kitao, H. Nakai, M. Klene, X. Li, J. E. Knox, H. P. Hratchian, J. B. Cross, V. Bakken, C. Adamo, J. Jaramillo, R. Gomperts, R. E. Stratmann, O. Yazyev, A. J. Austin, R. Cammi, C. Pomelli, J. W. Ochterski, P. Y. Ayala, K. Morokuma, G. A. Voth, P. Salvador, J. J. Dannenberg, V. G. Zakrzewski, S. Dapprich, A. D. Daniels, M. C. Strain, O. Farkas, D. K. Malick, A. D. Rabuck, K. Raghavachari, J. B. Foresman, J. V. Ortiz, Q. Cui, A. G. Baboul, S. Clifford, J. Cioslowski, B. B. Stefanov, G. Liu, A. Liashenko, P. Piskorz, I. Komaromi, R. L. Martin, D. J. Fox, T. Keith, M. A. Al-Laham, C. Y. Peng, A. Nanayakkara, M. Challacombe, P. M. W. Gill, B. Johnson, W. Chen, M. W. Wong, C. Gonzalez, J. A. Pople, *Gaussian 03*, revision D.01; *Gaussian, Inc.*: Wallingford, CT, 2004.
21 P. J. Hay and W. R. Wadt, *J. Chem. Phys.*, 1985, **82**, 270–283.

